Published in final edited form as:
Exp Neurol. 2013 December ; 250: . doi:10.1016/j.expneurol.2013.10.003.

Partial neuroprotection by nNOS inhibition during profound asphyxia in preterm fetal sheep

Paul P. Drury, BSc(Hons)[a], **Joanne O. Davidson, PhD**[a], **Lotte G. van den Heuij, MSc**[a], **Sidhartha Tan, MD**[b], **Richard B. Silverman, PhD**[c], **Haitao Ji, PhD**[c,d], **Arlin B. Blood, PhD**[e], **Mhoyra Fraser, PhD**[a,f], **Laura Bennet, PhD**[a], and **Alistair Jan Gunn, MBChB, PhD**[a]

[a]Department of Physiology, University of Auckland, Auckland, New Zealand (p.drury@auckland.ac.nz, joanne.davidson@auckland.ac.nz, l.vandenheuij@auckland.ac.nz, m.fraser@auckland.ac.nz, l.bennet@auckland.ac.nz, aj.gunn@auckland.ac.nz) [b]Department of Pediatrics, NorthShore University HealthSystem, Evanston, Ill. (sidtan@uchicago.edu) [c]Department of Chemistry, Department of Molecular Biosciences, Chemistry of Life Processes Institute, and Center for Molecular Innovation and Drug Discovery, Northwestern University, Evanston, IL 60208-3113 USA (r-silverman@northwestern.edu, markji@chem.utah.edu) [d]Department of Chemistry, University of Utah, Salt Lake City, UT, USA [e]Division of Neonatology, Department of Pediatrics, Loma Linda University School of Medicine, Loma Linda, CA, USA (ABBlood@llu.edu) [f]Liggins Institute, University of Auckland, Auckland, New Zealand

Abstract

Preterm brain injury is partly associated with hypoxia-ischemia starting before birth. Excessive nitric oxide production during HI may cause nitrosative stress, leading to cell membrane and mitochondrial damage. We therefore tested the hypothesis that therapy with a new, selective neuronal nitric oxide synthase (nNOS) inhibitor, JI-10 (0.022 mg/kg bolus, n=8), given 30 min before 25 min of complete umbilical cord occlusion was protective in preterm fetal sheep at 101-104 d gestation (term is 147 d), compared to saline (n=8). JI-10 had no effect on fetal blood pressure, heart rate, carotid and femoral blood flow, total EEG power, nuchal activity, temperature or intracerebral oxygenation on near-infrared spectroscopy during or after occlusion. JI-10 was associated with later onset of post-asphyxial seizures compared with saline ($p<0.05$), and attenuation of the subsequent progressive loss of cytochrome oxidase ($p<0.05$). After 7 days recovery, JI-10 was associated with improved neuronal survival in the caudate nucleus ($p<0.05$), but not the putamen or hippocampus, and more CNPase positive oligodendrocytes in the periventricular white matter ($p<0.05$). In conclusion, prophylactic nNOS inhibition before profound asphyxia was associated with delayed onset of seizures, slower decline of cytochrome oxidase and partial white and grey matter protection, consistent with protection of mitochondrial function.

Correspondence: Professor Alistair Jan Gunn MBChB, PhD Departments of Physiology and Paediatrics, Faculty of Medical and Health Sciences, The University of Auckland, Private Bag 92019, Auckland 1023, New Zealand aj.gunn@auckland.ac.nz Fax: (649) 373 7499 Phone: (649)373 7599 ext 86763 .

Disclosure/conflict of interest: JI-10 is under patent by R.B.S. US 7,994,326 B2. All other authors report no conflict of interest.

Keywords

Asphyxia; brain; nNOS; neuroprotection; preterm fetus

Introduction

Cerebral palsy (CP) of perinatal origin remains a major problem (Committee on Understanding Premature Birth and Assuring Healthy Outcomes, 2007). There is increasing evidence that it results from antenatal hypoxia-ischemia (HI) in about 70-80 % of the cases (Graham, et al., 2008), particularly around premature birth (Robertson, et al., 2007). Numerous preclinical studies have implicated reactive oxygen species in the pathogenesis of preterm brain injury. $NO^{\bullet}$ generation by neuronal nitric oxide synthase (nNOS) is increased during and after HI (Wei, et al., 1999). Reaction of $NO^{\bullet}$ with superoxide in the cytosol and mitochondria produces peroxynitrite and other reactive nitrogen species that are associated with cell membrane, organelle and mitochondrial damage (Tan, et al., 1999).

Combined inhibition of nNOS and inducible NOS (iNOS) with 2-iminobiotin (2-IB) in full term piglets immediately after severe HI is associated with short-term reduction in neuronal death (Peeters-Scholte, et al., 2002a). However, others have reported that although 2-IB was associated with increased survival with a normal aEEG (Bjorkman, et al., 2013), there was no improvement in neurobehavioral recovery, caspase-3 activity in thalamus, or histological damage, suggesting relatively limited benefit from post-insult treatment. Given the importance of intra-insult NO generation, it is possible that prophylactic treatment would be needed for optimal effect.

Supporting this concept, selective nNOS inhibition during prenatal asphyxia was associated with reduced CP in rabbit kits (Ji, et al., 2009, Yu, et al., 2011). Further, nNOS inhibition preserved mitochondrial membrane integrity and function whereas inhibition of iNOS was ineffective (Rao, et al., 2011). These promising findings using two previous iterations of nNOS inhibitors suggested further testing of the concept in a translational large animal model.

In the present study, we tested the hypothesis that prophylactic selective inhibition of nNOS with a new highly specific inhibitor, JI-10, would be neuroprotective following profound asphyxia in 0.7 gestation preterm fetal sheep, when brain development is broadly consistent with 28 to 32 weeks gestation in humans, before the development of cortical myelination (McIntosh, et al.). This is a well characterised paradigm that allows long-term, real-time monitoring of many physiological parameters including brain activity and temperature, carotid artery blood flow, heart rate, blood pressure and body movements (Bennet, et al., 2007, Drury, et al., 2012, Drury, et al., 2013). We investigated JI-10 in this study given its better bio-availability compared to JI-8 or HJ619 that were tested before in rabbits (Ji, et al., 2009, Yu, et al., 2011).

Methods

All procedures were approved by the Animal Ethics Committee of The University of Auckland, following the New Zealand Animal Welfare Act, and the Code of Ethical Conduct for animals in research established by the Ministry of Primary Industries, Government of New Zealand.

Twenty-four Romney/Suffolk fetal sheep were operated on at 98-99 days of gestation (term = 147 days). Food, but not water was withdrawn 18 h before surgery. Ewes were given 5 ml

of Streptocin (procaine penicillin (250,000 IU) and dihydrostreptomycin (250 mg/ml); Stockguard Labs Ltd, Hamilton, N.Z.) intramuscularly 30 min prior to the start of surgery. Maternal weight was recorded. Anesthesia was induced by i.v. injection of propofol (5 mg/kg; AstraZeneca Limited, Auckland, New Zealand), and general anesthesia maintained using 2-3% isoflurane in O_2. Under anesthesia, a 20 g i.v. catheter was placed in a maternal front leg vein and the ewes were placed on a constant infusion saline drip to maintain maternal fluid balance. Ewes were ventilated, and the depth of anesthesia, maternal heart rate and respiration were constantly monitored by trained anesthetic staff.

As previously described (Bennet, et al., 1999), catheters were placed in the left fetal femoral artery and vein, right brachial artery and vein, and the amniotic sac. A 3S ultrasonic blood flow probe (Transonic Systems Inc., Ithaca, NY, USA) was placed around the left carotid artery to measure carotid blood flow (CaBF) as an index of global cerebral blood flow (Bennet, et al., 1999, Gonzalez, et al., 2005, van Bel, et al., 1994), and a 2R probe was placed around the femoral artery to measure femoral blood flow (FBF). EEG electrodes (AS633-5SSF, Cooner Wire Co., Chatsworth, CA, USA) were placed on the dura over the parasagittal parietal cortex (5 mm and 10 mm anterior to bregma and 5 mm lateral). To measure cortical impedance a third pair of electrodes was placed over the dura 5 mm lateral to the EEG electrodes. Electrodes were placed to measure nuchal electromyography (EMG) and the fetal electrocardiogram (ECG). An inflatable silicone occluder was placed around the umbilical cord of all fetuses (In Vivo Metric, Healdsburg, CA, USA). Two small flexible fiber optic probes used for the near infrared spectroscopy recordings were placed biparietally on the skull 3.0 to 3.5 cm apart, 1.5 cm anterior to bregma, and secured using rapid setting dental cement (Rocket Red, Dental Adventures of America, Inc., Anaheim, CA, USA). All fetal leads were exteriorized through the maternal flank and a maternal long saphenous vein was catheterized to provide access for post-operative care and euthanasia. Gentamicin (80 mg, Rousell, Auckland, New Zealand) was administered into the amniotic fluid after the uterus was closed.

Post-operatively all sheep were housed in separate metabolic cages with access to water and food *ad libitum*, together in a temperature-controlled room (16±1 °C, humidity 50±10 %) with a 12 h light/dark cycle. A period of at least 4 days post-operative recovery was allowed before experiments commenced, during which time antibiotics were administered i.v. to the ewe daily for four days (600 mg benzylpenicillin sodium; Novartis Ltd, Auckland, New Zealand, and 80 mg gentamicin). Fetal catheters were maintained patent by continuous infusion of heparinized saline (20 U/ml at 0.15 ml/h) and the maternal catheter maintained by daily flushing. JI-10 was dissolved with sterile 0.9% saline (0.022 mg/ml) and a total of 0.066 mg was given, to achieve 100x the Ki of 0.0077 μmol/l shown in previous experiments (Ji, et al., 2010), with estimated fetal weight 1.5 kg, and a circulating fetal blood volume of 120 ml/kg. All containers and syringes for JI-10 were first rinsed with 10 % bovine serum albumin in sterile saline, after filtering through a bacterial filter.

Recordings

Fetal mean arterial blood pressure (MAP, Novatrans II, MX860; Medex Inc., Hilliard, OH, USA), corrected for maternal movement by subtraction of amniotic fluid pressure, fetal heart rate (FHR) derived from the ECG, CaBF, FBF, EEG, cortical impedance, and EMG were recorded continuously from −24 h to 168 h after umbilical cord occlusion. The blood pressure signal was collected at 64 Hz and low pass filtered at 30 Hz. The nuchal EMG signal was band-pass filtered between 100 Hz and 1 kHz, the signal was then integrated using a time constant of 1 sec. The analogue fetal EEG signal was low pass filtered with the cut-off frequency set with the −3 dB point at 30 Hz, and digitized at 256 Hz (using analogue to digital cards, National Instruments Corp., Austin, TX, USA). The intensity and frequency

were derived from the intensity spectrum signal between 0.5 and 20 Hz. For data presentation, the total EEG intensity (power) was normalized by log transformation (dB, 20 × log (intensity)), and data from left and right EEG electrodes were averaged. Power in the delta (0-3.9 Hz), theta (4-7.9 Hz), alpha (8-12.9 Hz), and beta (13-22 Hz) spectral bands was calculated, as previously described (Keogh, et al., 2012a).

Near-infrared spectroscopy (NIRS) measurements

Concentration changes in fetal cerebral deoxyhemoglobin ([Hb]), oxyhemoglobin ([HbO_2]) and oxidized cytochrome oxidase (CytOx) were measured using a NIR 500 spectrophotometer (Hamamatsu Photonics KK, Hamamatsu City, Japan) and data recorded by computer for off-line analysis (Drury, et al., 2012). The NIRS measures are relative changes from zero. Two key parameters were calculated: total hemoglobin ([THb]): the sum of [HbO_2] and [Hb], and delta Hb ([DHb]: the difference between [HbO_2] and [Hb]). THb is related to cerebral blood volume (CBV) by the cerebral hematocrit: CBV = [THb]/(Hct X R) where Hct is the arterial hematocrit and R is the cerebral-to-large vessel hematocrit ratio, assumed to be 0.69 (Wyatt, et al., 1990). THb is as an index of CBV given a stable blood hemoglobin and hematocrit (van Bel, et al., 1993). DHb is a measure of relative cerebral intravascular oxygenation (Brun, et al., 1997).

Experimental protocol

Experiments were conducted at 103-104 days gestation. Fetuses were randomly assigned to JI-10+occlusion (n = 8) or saline+occlusion (n = 8). Sham occlusion fetuses received no occlusion (n = 8). JI-10 dissolved in normal saline was administered to the fetal brachial vein 15 min prior to umbilical cord occlusion as a 3 ml dose of 0.022 mg/ml, over 10 min; saline+occlusion fetuses received the same volume of saline.

Fetal asphyxia was induced by rapid inflation of the umbilical cord occluder for 25 min with sterile saline of a defined volume known to completely inflate the occluder. Successful occlusion was confirmed by observation of a rapid onset of bradycardia, and by pH and blood gas measurements. The duration of occlusion was chosen as one that we have previously reported to represent an acute, severe, near-terminal insult but which could be survived without post-asphyxial cardiac support, and is associated with severe subcortical neuronal loss (Bennet, et al., 2007). All occlusions or sham occlusions were undertaken around 0900 h.

Fetal arterial blood was taken at 30 min prior to occlusion, 5 and 17 min during asphyxia, and then 10 min, 1, 2, 4, 6, 24, 48, 72, 96, 120, 144, and 168 h post-asphyxia for pH and blood gas determination (Ciba-Corning Diagnostics 845 blood gas analyzer and co-oximeter, MA., USA) and for glucose and lactate measurements (YSI model 2300, Yellow Springs, Ohio, USA). Samples at −30 min prior to occlusion, at + 6 h, and then daily samples from the day after occlusion at 0900 were taken for plasma cortisol, ACTH, and melatonin concentration determination.

Ewes and fetuses were killed 7 days after occlusion by intravenous overdose of pentobarbitone sodium (9 g) to the ewe (Pentobarb 300; Chemstock International, Christchurch, New Zealand). At post-mortem, fetuses were examined for the presence of ascites, defined as easy aspiration of > 5 mL peritoneal fluid. Sub-cutaneous edema was measured over the fetal shoulders, flank, and abdomen with calipers.

Hormone assays

Cortisol levels were measured by a liquid chromatography-tandem mass spectrometry method. In brief, 200 μL of plasma samples were mixed in a glass tube with 100 μL of

deuterium labeled internal standard [20 ng/mL cortisol-d_4 (Cambridge Isotope Laboratory, MA, USA) in water]. 1 mL of ethyl acetate (Merck KGaA, Darnstadt, Germany) was then added to the tubes and vortexed for 30 s. The samples were then centrifuged for 10 min, and the organic phase was collected in collection glass tubes and lyophilized with the help of a freeze drier. The extract was re-dissolved in 60 μL of mobile phase (72 % methanol and 28 % water) and transferred to 200 μL PVC inserts in HPLC vials. A total of 12 μl of sample was injected to the auto sampler. The HPLC system (Alliance 2690; Waters Corp., Milford, MA) was interfaced to a triple quadrupole mass spectrometer (Finnigan TSQ Quantum Ultra AM, Thermo Electron Corp, San Jose, CA). The parent-to-daughter ion transition for cortisol was 363.2-122.2 at 28 V and for cortisol-d_4 it was 367.2 – 121.2. The retention time was 3.1 min for cortisol and cortisol-d_4. The data were analyzed using Finnigan Excalibur software (Thermo Electron Corp). Mean inter and intra assay CV values for cortisol were 5.8 and 6.0 %, respectively.

ACTH levels in the plasma samples were measured in duplicate using a 125I RIA kit (24130, DiaSorin, Stillwater, MN) validated for ovine maternal and fetal plasma. The intra-assay coefficient of variation was 9.7 % and the inter-assay coefficient was 12.8 %. The mean ACTH assay sensitivity was 9.7 pg/mL and samples showing less than this value were assigned this value for analysis.

For plasma nitrite levels 300 μl of plasma was deproteinized by addition of an equal volume of methanol followed by vortexing and centrifugation for 10 min at 14,000 rcf. The supernatant was then injected into a purge vessel containing acidified triiodide solution to reduce nitrite to NO as previously described (Blood and Power, 2007). The triiodide was sparged with a stream of argon gas, which carried the resulting NO gas into a chemiluminescence analyzer (Sievers 280i NO Analyzer, GE Analytical Instruments, Boulder, CO, USA). Nitrite concentrations were quantified by comparison with injections of known nitrite standards. The assay enables quantification of nitrite concentrations above 10 nM with a precision of ± 5 nM, and does not detect nitrate at concentrations below 1 mM.

Histopathology

At post-mortem, 7 days after occlusion, the fetal brains were perfusion fixed with 10 % phosphate-buffered formalin. Slices (10 μm thick) were cut using a microtome (Leica Jung RM2035). Slides were dewaxed in xylene and rehydrated in decreasing concentrations of ethanol. Slides were washed in 0.1 mol/L phosphate buffered saline (PBS). Antigen retrieval was performed using the citrate buffer boil method and endogenous peroxidase quenching was performed by incubation in 1 % H_2O_2 in methanol for anti-neuronal nuclei monoclonal antibody (NeuN), Iba-1, CNPase, and Ki-67 and in PBS for Olig-2. Blocking was performed in 3 % normal horse serum (NHS) for NeuN and Iba-1 and normal goat serum (NGS) for Olig-2, CNPase and Ki-67 for 1 h at room temperature. Sections were labeled with 1:400 mouse NeuN (Chemicon International, Temecula, CA, USA) 1:400 Olig-2 (Chemicon International, Olig-2, a marker for oligodendrocytes at all stages of the lineage (Jakovcevski, et al., 2009)), 1:200 ki-67 (Dako, Aus), 1:200 goat anti-Iba-1 (Abcam) and 1:200 mouse anti-CNPase (Abcam) overnight at 4 °C. Sections were incubated in biotin-conjugated secondary 1:200 horse anti-mouse (NeuN) or 1:200 goat anti-rabbit IgG (Vector Laboratories, Burlingame, USA) in 3.5% NHS for 2 h at room temperature. Slides were then incubated in ExtrAvidin® (1:200, Sigma-Aldrich Pty. Ltd.) in PBS for 2 h at room temperature and then allowed to react in diaminobenzidine tetrachloride (DAB) (Sigma-Aldrich Pty. Ltd.). The reaction was stopped by washing in dH_2O, the sections dehydrated and mounted. For fluorescent double labeling, dewaxing, rehydrating and antigen retrieval was performed as described above. Sections were blocked in 3% NGS for 1 h at room temperature. Sections were incubated with 1:400 rabbit anti-Olig-2 and 1:200 mouse anti-

Ki-67 in 3% NGS at 4° C overnight. Sections were washed in PBS and incubated with 1:200 biotinylated goat anti-mouse IgG (Vector Laboratories) for 3 h at room temperature. Sections were washed and incubated with 1:200 streptavidin Alexa 488 and 1:200 donkey anti-rabbit Alexa 568.

Brain regions of the forebrain used for analysis included the mid-striatum (comprising the caudate nucleus and putamen) and the frontal subcortical white matter (comprising the intragyral, IGWM, and periventricular, PVWM, regions) on sections taken 23 mm anterior to stereotaxic zero. The cornu ammonis (CA) of the dorsal horn of the anterior hippocampus (divided into CA1/2, CA3, CA4, and dentate gyrus (DG)) were assessed on sections taken 17 mm anterior to stereotaxic zero. Neuronal (NeuN), oligodendrocyte (Olig-2, CNPase) and microglial (Iba-1) changes, and proliferation (Ki-67) were scored on stained sections by light microscopy at x40 magnification on a Nikon 80i microscope and NIS Elements Br 4.0 software (Nikon Instruments Inc., Melville, N.Y., U.S.A.) using seven fields in the striatum (four in caudate nucleus, three in putamen), two fields in the white matter (one intragyral, one periventricular), and one field in each of the hippocampal divisions as previously described (Dean, et al., 2006). Total microglia were counted as all cells with Iba-1 immunostaining. For assessment of activated microglia Iba-1 cells showing an amoeboid morphology with no cell processes were counted. For each animal, average scores across both hemispheres from two sections were calculated for each region. Counts were made by an assessor blinded to the treatment groups.

Data analysis

Off-line analysis of the physiological data was performed using customized Labview programs. The raw EEG was assessed for epileptiform activity. Seizures were identified visually and defined as the concurrent appearance of sudden, repetitive, evolving stereotyped waveforms in the EEG signal lasting more than 10 sec and of an amplitude greater than 20 μV (Scher, et al., 1993).

Data were analyzed using SPSS 15.0 for Windows (SPSS, Chicago, Il, USA) and JMP 8.0 (SAS Institute, Cary, North Carolina, USA). For analysis of recovery data after occlusion (from 1 to 168 h post-occlusion) the baseline period was taken as the mean of the 24 h before occlusion. For between group comparisons two-way analysis of variance (ANOVA) for repeated measures was performed. When statistical significance was found between groups for repeated measures ANOVA in JMP post-hoc contrast tests were used between groups. Where significance was found between group and time for repeated measures, or over time by one-way ANOVA, Tukey's pairwise comparisons were used to compare selected time points. For blood gas, electrolyte, LFT, hormonal, and histological data ANOVA was performed, and where significance was found, followed by post-hoc Tukey's pairwise comparisons. Where baseline differences were found, analysis of covariance was performed on subsequent results with least-squares difference post-hoc tests as appropriate. Non-parametric Mann-Whitney U-tests were used where appropriate. Fishers' Exact test was used to compare the presence of ascites. Statistical significance was accepted as $p < 0.05$. Data are presented as mean ± SEM unless otherwise stated.

Results

Baseline and umbilical cord occlusion

Baseline blood gases, acid-base status and glucose-lactate values were not different between groups (Table 1). Umbilical cord occlusion was associated with marked fetal hypoxia, hypercarbia, and acidosis (Table 1), bradycardia, hypotension, peripheral vasoconstriction,

cerebral hypoperfusion, EEG suppression, increased cortical impedance, with a profound reduction in HbO_2 and reciprocally increased Hb on NIRS measurement (Figure 1).

The pH and oxygen content were significantly lower in the JI-10+occlusion group at +10 min after occlusion ($p < 0.05$). There were no other cardiovascular, neurophysiological or biochemical differences between groups during or in the immediate post-occlusion period. CaBF showed a statistically borderline reduction in the JI-10+occlusion group from 2 to 3 h compared to saline+occlusion ($p = 0.05$).

Recovery

EEG power was suppressed for more than 36 h in both groups, with similar loss of high frequency activity in both groups, before progressively recovering to baseline values by approximately 96 h. Electrographic seizures developed median (interquartile range) 354 (329-403) min after saline+occlusion, with a marked further delay after JI-10+occlusion (588 (453-895) min, $p < 0.05$, Figure 2). Consistent with reduced seizures, JI-10+occlusion was associated with transiently reduced low frequency power in this interval (delta band at 6 and 7 h, theta band at 7 h and alpha band at 10-12 h, Figure 2, $p<0.05$) and a transient reduction in nuchal EMG activity from 39–48 h (Supplementary figure 1, $p<0.05$). However, there was no significant difference in number, duration, or peak amplitude of individual seizures.

There were no significant differences between groups for MAP, FHR, extra-dural temperature, CaBF, CVC, FBF, FVC, or impedance (Supplementary figures 1 and 2).

Near-infrared spectroscopy

After occlusion, there was rapid recovery of intracerebral oxygenation. Approximately 2 h after recovery, there was marked, persistent reduction in THb in both groups, accompanied by a transient reduction in DHb, suggesting a period of relative hypoperfusion. This was followed by a marked, persistent secondary increase from 6 h consistent with relative hyperperfusion that was not different between groups. The JI-10 group showed a statistically borderline reduction in both THb ($p = 0.05$; significant from 1 to 6 h) and HbO_2 during recovery compared to saline ($p = 0.05$; Figure 2).

CytOx recovered rapidly after occlusion in both groups. JI-10+occlusion was associated with a transient increase in the first few hours compared to the saline+occlusion, which was significant after 3 h. In both groups CytOx then progressive fell below baseline values. This fall was slower after JI-10+occlusion (Figure 2, $p < 0.05$) and overall, CytOx values were higher throughout the 72 h recovery after JI-10+occlusion compared to saline+occlusion ($p<0.05$).

Biochemistry

The profound mixed respiratory and metabolic acidosis associated with occlusion progressively resolved after occlusion in both groups (Table 1, $p < 0.05$). There were only minor differences in any measured value between groups over the 7 days recovery (Table and Supplementary table 1).

Plasma nitrite values were not significantly different between groups at any time. Plasma nitrite was significantly higher than baseline in the JI-10+occlusion group at 5 min and 17 min during occlusion, and at +10 min after occlusion (Table 1, $p < 0.05$), whereas the vehicle-occlusion group was never significantly different from baseline at any point. Plasma ACTH and cortisol increased after occlusion, with similar elevations at +6 h and +24 h in both groups (Supplementary table 1).

Post-mortem

Body weight was significantly greater in the JI-10+occlusion group compared to sham occlusion (Supplementary table 2, $p < 0.05$), and adrenal weight was significantly greater after JI-10+occlusion compared to saline+occlusion ($p < 0.05$). Ascites and edema were not seen in sham-occluded fetuses. Frank intrapleural ascites was seen in 5/8 fetuses in the JI-10+occlusion group compared to 2/8 in the saline+occlusion group ($p = 0.3$). Sub-cutaneous edema was 8 (5-10, median (range)) mm in the JI-10+occlusion group compared to 2 (0-4) mm in the saline+occlusion group ($p < 0 .05$). Flank sub-cutaneous edema was 8 (0-15) mm in the JI-10 group and 1 (0-6) mm in the saline group. Abdominal sub-cutaneous edema was 5 (0-13) mm in the JI-10 group and 0 (0-10) mm in the saline group.

Histopathology

Occlusion was associated with marked (NeuN positive) neuronal loss in the basal ganglia and the CA1-2 and CA2 regions of the hippocampus compared to sham controls (Figure 3 $p < 0.05$). JI-10+occlusion was associated with significantly greater neuronal survival in the caudate nucleus, but no effect in the putamen or hippocampal regions.

There was no effect of occlusion or JI-10 on numbers of Olig-2 positive cells in the white matter tracts (Figure 5), whereas there was a marked reduction in numbers of staining for CNPase positive (immature/mature) oligodendrocytes after saline+occlusion. JI-10 was associated with a significant increase in CNPase positive cells in PVWM but not the IGWM compared to sham occlusion ($p < 0.05$). There was a similar increase in Ki-67 positive proliferating cells and Iba-1 positive microglia in the IGWM and PVWM in both occlusion groups ($p < 0.05$). Ki-67 immunofluorescent cells frequently co-localized with Olig-2 (Supplementary Figure 3).

Discussion

The present study demonstrates that in preterm fetal sheep prophylactic selective inhibition of nNOS, using JI-10 with a Ki of 8 nM, was associated with a delay in the onset of seizures and attenuated secondary mitochondrial failure, with partial neuronal and white matter protection after 7 days recovery. Encouragingly, there was no increase in mortality after nNOS inhibition. However, there was a statistically borderline reduction in fetal THb, a measure of intracerebral hemoglobin content and of carotid blood flow that suggests residual nonspecific inhibition of endothelial NOS (eNOS) (Peeters-Scholte, et al., 2002b). Further, nNOS inhibition was associated with increased fetal weight and greater subcutaneous edema, consistent with greater extracellular fluid retention.

NO rapidly and reversibly inhibits CytOx by binding to the reduced form in competition with oxygen (Sarti, et al., 2012). Consistent with this, although JI-10 did not affect CytOx during asphyxia, it was associated with a greater rebound increase in oxidized CytOx 3 h after occlusion, suggesting reduced inhibition by NO. Previous studies have shown reduced nNOS activity immediately after HI, but not at +24 h in rabbit kits following bolus doses of a related NOS inhibitor before and after uterine ischaemia (Yu, et al., 2011). We cannot exclude the possibility that continuing post-insult therapy might have increased benefit by maintaining inhibition (Rao, et al., 2011). However, repeated dosing with 2-IB until 20 h after HI in the piglet was associated with no significant improvement in histological damage (Bjorkman, et al., 2013), supporting the general concept that nNOS activity primarily contributes to injury in the immediate perinatal insult phase.

In the present study JI-10 was associated with attenuation of the progressive loss of CytOx after occlusion. The CytOx signal measured by NIRS closely correlates with changes in oxidised cytochrome oxidase in the piglet during cyanide induced reduction (Cooper, et al.,

1999), and with loss of oxidative metabolism measured by magnetic resonance spectroscopy after hypoxia-ischemia (Cooper, 1999). In many settings, persistent loss of CytOx reflects cell loss. For example, the magnitude of the fall is related to improved outcome in human infants (van Bel, et al., 1993), and greater loss of CytOx during recovery was associated with worse injury in piglets after deep hypothermic circulatory arrest (Shum-Tim, et al., 1998). In the current paradigm, the onset of secondary loss of CytOx coincides with the onset of seizures (Bennet, et al., 2006). There is some evidence linking neuronal NO production to NMDA receptor activation (Ledo, et al., 2005), and thus inhibition with JI-10 may have been associated with reduced excitatory signaling. In near-term fetal sheep, infusion of L-nitroarginine, an inhibitor of all NOS isoforms, from 2-72 h after 30 min cerebral ischemia, was not associated with a change in the secondary CytOx decline or a delay in seizure onset, but was associated with a longer duration of seizures, and with increased neuronal injury, possibly by impairing cerebral perfusion (Marks, et al., 1996). Taken as a whole, these studies suggest that prophylactic NOS inhibition is more beneficial than post-insult inhibition

Histologically, treatment before asphyxia with JI-10 was associated with neuronal protection in the caudate nucleus but not other grey matter regions, and substantial improvement in numbers of immature/mature oligodendrocytes in the PVWM. Given that we found no significant cortical injury, it is likely that post-occlusion seizures arise from subcortical regions, and thus the reduced injury of the caudate likely contributed to delayed onset of secondary seizures in this study (Gunn and Bennet, 2010). It is unknown why JI-10 did not protect the hippocampal regions; however, the hippocampus is typically one of the most vulnerable regions to hypoxia-ischemia (Keogh, et al., 2012b, Williams, et al., 1992). Given that more severe insults typically lead to more rapid evolution of injury with less effect of treatment (Sabir, et al., 2012), we speculate that greater and more rapidly evolving injury in the hippocampus may reduce the potential for benefit from nNOS blockade.

There was no effect of asphyxia or nNOS inhibition on total numbers of oligodendrocytes, but a marked increase in Ki-67 immunostaining, which was substantially co-localized with Olig-2. Olig-2 is a marker for all cells in the oligodendrocyte lineage; however, the exuberant proliferation response to injury is almost entirely mediated by oligodendrocyte progenitor cells (Baumann and Pham-Dinh, 2001). We have previously shown that asphyxia is associated with marked loss of pre-oligodendrocytes after 3 days recovery (Barrett, et al., 2012). This combination of findings is consistent with the hypothesis that occlusion was associated with early cell loss, followed by restorative proliferation and subsequent maturational arrest, consistent with foundational studies from Back and colleagues in preterm human infants (Segovia, et al., 2008). This suggests that the improved recovery of immature/mature oligodendrocytes in the present study reflects alleviation of maturation arrest rather than direct cell protection.

MAP, peripheral blood flow and conductance, and plasma nitrite were not different between groups, and the JI-10 group showed only transiently lower pH, 10 min after occlusion, suggesting that JI-10 had minimal systemic effects. There was no effect of JI-10 on intracerebral oxygenation as measured by DHb, suggesting that there was no effect on oxygen delivery, consistent with the apparent safety of less potent nNOS inhibitors in the fetal rabbit (Yu, et al., 2011). There was a statistically borderline reduction in THb. Given that NIRS primarily interrogates the venous compartment, combined with lack of effect on oxygenation, we may infer that JI-10 led to relative veno-constriction. Although nitrite levels, which serve as an index of eNOS activity (Kleinbongard, et al., 2003), were not different between groups, the most likely explanation is a minor degree of nonspecific inhibition of eNOS.

Moreover, at post-mortem there was greater total body weight after JI-10+occlusion. Combined with the significant increase in subcutaneous edema, this denotes positive fluid balance. Given that there were no differences in plasma electrolytes or protein, it is unlikely that this reflects an oncotic effect. Further, fetal heart rate and MAP were not altered and central venous pressure was not increased, and so there was no evidence of impaired cardiac function. Potentially, for example nNOS inhibition could exacerbate the dramatic fall in renal blood flow and urine output that occur after asphyxia (Quaedackers, et al., 2004). Although NO does have an important role in an inhibiting sympathetic outflow from the paraventricular nucleus (Li, et al., 2001), there was no change in renal sympathetic nerve activity following NO blockade with L-NAME in rabbits (Ramchandra, et al., 2007). Alternatively, fetal hypoxia is associated with altered eNOS-dependent relaxation of umbilical vessels, with increased eNOS expression in umbilical arteries and reduced eNOS in the umbilical veins (Hracsko, et al., 2009), regulated at least in part by greater arginase-2 production in the umbilical venous circulation, reducing eNOS activity (Krause, et al., 2013). Further studies are needed to assess whether JI-10 could modulate these differential responses to hypoxia to alter the net hydrostatic pressure difference across the placenta and so promote fetal fluid accumulation (Lumbers, et al., 2001).

In conclusion, the present findings that selective inhibition of nNOS did not compromise fetal adaptation during profound asphyxia and was partially protective, suggest that with further safety testing, this may be a viable therapeutic strategy for at risk preterm deliveries. The observation that nNOS inhibition delayed secondary seizures and mitochondrial failure raises the intriguing possibility that this strategy may increase the window of opportunity for other complementary neuroprotective strategies, such as the free radical antagonist and anti-inflammatory agent, melatonin (Drury, et al., 2013, Robertson, et al., 2013), and anti-apoptotic therapies such as EPO (Robertson, et al., 2012).

Supplementary Material

Refer to Web version on PubMed Central for supplementary material.

Acknowledgments

Funding. This study was supported by NIH grants R21 NS063141-01A1 (ST, AG, LB), R01 GM049725 (RBS), 2R56 NS043285, R01 NS051402 (ST) and HL095973 (A.B.B.), the Health Research Council of New Zealand, the Auckland Medical Research Foundation and the Lottery Health Grants Board of New Zealand. P Drury was supported by the New Zealand Neurological Foundation W&B Miller Doctoral Scholarship.

References

1. Barrett RD, Bennet L, Naylor A, George SA, Dean JM, Gunn AJ. Effect of cerebral hypothermia and asphyxia on the subventricular zone and white matter tracts in preterm fetal sheep. Brain Res. 2012; 1469:35–42. [PubMed: 22765912]
2. Baumann N, Pham-Dinh D. Biology of oligodendrocyte and myelin in the mammalian central nervous system. Physiol. Rev. 2001; 81:871–927. [PubMed: 11274346]
3. Bennet L, Roelfsema V, George S, Dean JM, Emerald BS, Gunn AJ. The effect of cerebral hypothermia on white and grey matter injury induced by severe hypoxia in preterm fetal sheep. J. Physiol. 2007; 578:491–506. [PubMed: 17095565]
4. Bennet L, Roelfsema V, Pathipati P, Quaedackers J, Gunn AJ. Relationship between evolving epileptiform activity and delayed loss of mitochondrial activity after asphyxia measured by near-infrared spectroscopy in preterm fetal sheep. J. Physiol. 2006; 572:141–154. [PubMed: 16484298]
5. Bennet L, Rossenrode S, Gunning MI, Gluckman PD, Gunn AJ. The cardiovascular and cerebrovascular responses of the immature fetal sheep to acute umbilical cord occlusion. J. Physiol. 1999; 517:247–257. [PubMed: 10226163]

6. Bjorkman ST, Ireland Z, Fan X, van der Wal WM, Roes KC, Colditz PB, Peeters-Scholte CM. Short-term dose-response characteristics of 2-iminobiotin immediately postinsult in the neonatal piglet after hypoxia-ischemia. Stroke. 2013; 44:809–811. [PubMed: 23362078]
7. Blood AB, Power GG. In vitro and in vivo kinetic handling of nitrite in blood: effects of varying hemoglobin oxygen saturation. Am. J. Physiol. Heart Circ. Physiol. 2007; 293:H1508–1517. [PubMed: 17513487]
8. Brun NC, Moen A, Borch K, Saugstad OD, Greisen G. Near-infrared monitoring of cerebral tissue oxygen saturation and blood volume in newborn piglets. Am. J. Physiol. 1997; 273:H682–686. [PubMed: 9277484]
9. Committee on Understanding Premature Birth and Assuring Healthy Outcomes. Preterm Birth: Causes, Consequences, and Prevention. Institute of Medicine, The National Academies Press; 2007. http://books.nap.edu//catalog/11622.html#toc
10. Cooper CE. In vivo measurements of mitochondrial function and cell death following hypoxic/ischaemic damage to the new-born brain. Biochem. Soc. Symp. 1999; 66:123–140. [PubMed: 10989663]
11. Cooper CE, Cope M, Springett R, Amess PN, Penrice J, Tyszczuk L, Punwani S, Ordidge R, Wyatt J, Delpy DT. Use of mitochondrial inhibitors to demonstrate that cytochrome oxidase near-infrared spectroscopy can measure mitochondrial dysfunction noninvasively in the brain. J. Cereb. Blood Flow Metab. 1999; 19:27–38. [PubMed: 9886352]
12. Dean JM, Gunn AJ, Wassink G, George S, Bennet L. Endogenous alpha(2)-adrenergic receptor-mediated neuroprotection after severe hypoxia in preterm fetal sheep. Neuroscience. 2006; 142:615–628. [PubMed: 16952424]
13. Drury PP, Bennet L, Booth LC, Davidson JO, Wassink G, Gunn AJ. Maturation of the mitochondrial redox response to profound asphyxia in fetal sheep. PLoS One. 2012; 7:e39273. [PubMed: 22720088]
14. Drury PP, Davidson JO, Bennet L, Booth LC, Tan S, Fraser M, van Den Heuij LG, Gunn AJ. Partial neural protection with prophylactic low-dose melatonin after asphyxia in preterm fetal sheep. J. Cereb. Blood Flow Metab. 2013 In press.
15. Gonzalez H, Hunter CJ, Bennet L, Power GG, Gunn AJ. Cerebral oxygenation during post-asphyxial seizures in near-term fetal sheep. J. Cereb. Blood Flow Metab. 2005; 25:911–918. [PubMed: 15729287]
16. Graham EM, Ruis KA, Hartman AL, Northington FJ, Fox HE. A systematic review of the role of intrapartum hypoxia-ischemia in the causation of neonatal encephalopathy. Am. J. Obstet. Gynecol. 2008; 199:587–595. [PubMed: 19084096]
17. Gunn AJ, Bennet L. Therapeutic hypothermia translates to the NICU. Semin. Fetal Neonatal Med. 2010; 15:237. [PubMed: 20558118]
18. Hracsko Z, Hermesz E, Ferencz A, Orvos H, Novak Z, Pal A, Varga IS. Endothelial nitric oxide synthase is up-regulated in the umbilical cord in pregnancies complicated with intrauterine growth retardation. Vivo. 2009; 23:727–732.
19. Jakovcevski I, Filipovic R, Mo Z, Rakic S, Zecevic N. Oligodendrocyte development and the onset of myelination in the human fetal brain. Front. Neuroanat. 2009; 3:5. [PubMed: 19521542]
20. Ji H, Delker SL, Li H, Martasek P, Roman LJ, Poulos TL, Silverman RB. Exploration of the active site of neuronal nitric oxide synthase by the design and synthesis of pyrrolidinomethyl 2-aminopyridine derivatives. J. Med. Chem. 2010; 53:7804–7824. [PubMed: 20958055]
21. Ji H, Tan S, Igarashi J, Li H, Derrick M, Martasek P, Roman LJ, Vasquez-Vivar J, Poulos TL, Silverman RB. Selective neuronal nitric oxide synthase inhibitors and the prevention of cerebral palsy. Ann. Neurol. 2009; 65:209–217. [PubMed: 19235180]
22. Keogh MJ, Bennet L, Drury PP, Booth LC, Mathai S, Naylor AS, Fraser M, Gunn AJ. Subclinical exposure to low-dose endotoxin impairs EEG maturation in preterm fetal sheep. Am. J. Physiol. Regul. Integr. Comp. Physiol. 2012a; 303:R270–278. [PubMed: 22696578]
23. Keogh MJ, Drury PP, Bennet L, Davidson JO, Mathai S, Gunn ER, Booth LC, Gunn AJ. Limited predictive value of early changes in EEG spectral power for neural injury after asphyxia in preterm fetal sheep. Pediatr. Res. 2012b; 71:345–353. [PubMed: 22391634]

24. Kleinbongard P, Dejam A, Lauer T, Rassaf T, Schindler A, Picker O, Scheeren T, Godecke A, Schrader J, Schulz R, Heusch G, Schaub GA, Bryan NS, Feelisch M, Kelm M. Plasma nitrite reflects constitutive nitric oxide synthase activity in mammals. Free Radic. Biol. Med. 2003; 35:790–796. [PubMed: 14583343]
25. Krause BJ, Carrasco-Wong I, Caniuguir A, Carvajal J, Farias M, Casanello P. Endothelial eNOS/arginase imbalance contributes to vascular dysfunction in IUGR umbilical and placental vessels. Placenta. 2013; 34:20–28. [PubMed: 23122700]
26. Ledo A, Barbosa RM, Gerhardt GA, Cadenas E, Laranjinha J. Concentration dynamics of nitric oxide in rat hippocampal subregions evoked by stimulation of the NMDA glutamate receptor. Proc. Natl. Acad. Sci. U. S. A. 2005; 102:17483–17488. [PubMed: 16293699]
27. Li YF, Mayhan WG, Patel KP. NMDA-mediated increase in renal sympathetic nerve discharge within the PVN: role of nitric oxide. Am. J. Physiol. Heart Circ. Physiol. 2001; 281:H2328–2336. [PubMed: 11709399]
28. Lumbers ER, Gunn AJ, Zhang DY, Wu JJ, Maxwell L, Bennet L. Nonimmune hydrops fetalis and activation of the renin-angiotensin system after asphyxia in preterm fetal sheep. Am. J. Physiol. Regul. Integr. Comp. Physiol. 2001; 280:R1045–R1051. [PubMed: 11247826]
29. Marks KA, Mallard CE, Roberts I, Williams CE, Gluckman PD, Edwards AD. Nitric oxide synthase inhibition attenuates delayed vasodilation and increases injury after cerebral ischemia in fetal sheep. Pediatr. Res. 1996; 40:185–191. [PubMed: 8827765]
30. McIntosh GH, Baghurst KI, Potter BJ, Hetzel BS. Foetal brain development in the sheep. Neuropathol. Appl. Neurobiol. 1979; 5:103–114. [PubMed: 471183]
31. Peeters-Scholte C, Koster J, Veldhuis W, van den Tweel E, Zhu C, Kops N, Blomgren K, Bar D, van Buul-Offers S, Hagberg H, Nicolay K, van Bel F, Groenendaal F. Neuroprotection by selective nitric oxide synthase inhibition at 24 hours after perinatal hypoxia-ischemia. Stroke. 2002a; 33:2304–2310. [PubMed: 12215603]
32. Peeters-Scholte C, van den Tweel E, Ioroi T, Post I, Braun K, Veldhuis W, Nicolay K, Groenendaal F, van Bel F. Pharmacological interventions in the newborn piglet in the first 24 h after hypoxia-ischemia. A hemodynamic and electrophysiological perspective. Exp. Brain Res. 2002b; 147:200–208. [PubMed: 12410335]
33. Quaedackers JS, Roelfsema V, Hunter CJ, Heineman E, Gunn AJ, Bennet L. Polyuria and impaired renal blood flow after asphyxia in preterm fetal sheep. Am. J. Physiol. Regul. Integr. Comp. Physiol. 2004; 286:R576–R583. [PubMed: 14604846]
34. Ramchandra R, Barrett CJ, Guild SJ, McBryde FD, Malpas SC. The role of renal sympathetic nerve activity in the hypertension induced by chronic nitric oxide inhibition. Am. J. Physiol. Regul. Integr. Comp. Physiol. 2007
35. Rao S, Lin Z, Drobyshevsky A, Chen L, Ji X, Ji H, Yang Y, Yu L, Derrick M, Silverman RB, Tan S. Involvement of neuronal nitric oxide synthase in ongoing fetal brain injury following near-term rabbit hypoxia-ischemia. Dev. Neurosci. 2011; 33:288–298. [PubMed: 21757865]
36. Robertson CM, Watt MJ, Yasui Y. Changes in the prevalence of cerebral palsy for children born very prematurely within a population-based program over 30 years. JAMA. 2007; 297:2733–2740. [PubMed: 17595274]
37. Robertson NJ, Faulkner S, Fleiss B, Bainbridge A, Andorka C, Price D, Powell E, Lecky-Thompson L, Thei L, Chandrasekaran M, Hristova M, Cady EB, Gressens P, Golay X, Raivich G. Melatonin augments hypothermic neuroprotection in a perinatal asphyxia model. Brain. 2013; 136:90–105. [PubMed: 23183236]
38. Robertson NJ, Tan S, Groenendaal F, van Bel F, Juul SE, Bennet L, Derrick M, Back SA, Valdez RC, Northington F, Gunn AJ, Mallard C. Which neuroprotective agents are ready for bench to bedside translation in the newborn infant? J. Pediatr. 2012; 160:544–552. e544. [PubMed: 22325255]
39. Sabir H, Scull-Brown E, Liu X, Thoresen M. Immediate hypothermia is not neuroprotective after severe hypoxia-ischemia and is deleterious when delayed by 12 hours in neonatal rats. Stroke. 2012; 43:3364–3370. [PubMed: 22996953]

40. Sarti P, Forte E, Mastronicola D, Giuffre A, Arese M. Cytochrome c oxidase and nitric oxide in action: molecular mechanisms and pathophysiological implications. Biochim. Biophys. Acta. 2012; 1817:610–619. [PubMed: 21939634]
41. Scher MS, Hamid MY, Steppe DA, Beggarly ME, Painter MJ. Ictal and interictal electrographic seizure durations in preterm and term neonates. Epilepsia. 1993; 34:284–288. [PubMed: 8453938]
42. Segovia KN, McClure M, Moravec M, Luo NL, Wan Y, Gong X, Riddle A, Craig A, Struve J, Sherman LS, Back SA. Arrested oligodendrocyte lineage maturation in chronic perinatal white matter injury. Ann. Neurol. 2008; 63:520–530. [PubMed: 18393269]
43. Shum-Tim D, Nagashima M, Shinoka T, Bucerius J, Nollert G, Lidov HG, du Plessis A, Laussen PC, Jonas RA. Postischemic hyperthermia exacerbates neurologic injury after deep hypothermic circulatory arrest. J. Thorac. Cardiovasc. Surg. 1998; 116:780–792. [PubMed: 9806385]
44. Tan S, Zhou F, Nielsen VG, Wang Z, Gladson CL, Parks DA. Increased injury following intermittent fetal hypoxia-reoxygenation is associated with increased free radical production in fetal rabbit brain. J. Neuropathol. Exp. Neurol. 1999; 58:972–981. [PubMed: 10499439]
45. van Bel F, Dorrepaal CA, Benders MJ, Zeeuwe PE, van de Bor M, Berger HM. Changes in cerebral hemodynamics and oxygenation in the first 24 hours after birth asphyxia. Pediatrics. 1993; 92:365–372. [PubMed: 8395685]
46. van Bel F, Roman C, Klautz RJ, Teitel DF, Rudolph AM. Relationship between brain blood flow and carotid arterial flow in the sheep fetus. Pediatr. Res. 1994; 35:329–333. [PubMed: 8190521]
47. Wei G, Dawson VL, Zweier JL. Role of neuronal and endothelial nitric oxide synthase in nitric oxide generation in the brain following cerebral ischemia. Biochim. Biophys. Acta. 1999; 1455:23–34. [PubMed: 10524226]
48. Williams CE, Gunn AJ, Mallard C, Gluckman PD. Outcome after ischemia in the developing sheep brain: an electroencephalographic and histological study. Ann. Neurol. 1992; 31:14–21. [PubMed: 1543346]
49. Wyatt JS, Cope M, Delpy DT, Richardson CE, Edwards AD, Wray S, Reynolds EO. Quantitation of cerebral blood volume in human infants by near-infrared spectroscopy. J. Appl. Physiol. 1990; 68:1086–1091. [PubMed: 2341336]
50. Yu L, Derrick M, Ji H, Silverman RB, Whitsett J, Vasquez-Vivar J, Tan S. Neuronal nitric oxide synthase inhibition prevents cerebral palsy following hypoxiaischemia in fetal rabbits: comparison between JI-8 and 7-nitroindazole. Dev. Neurosci. 2011; 33:312–319. [PubMed: 21659718]

Highlights

- The first large animal study of selective nNOS inhibition during asphyxia
- nNOS inhibition delayed onset of post-asphyxial seizures
- nNOS inhibition attenuated secondary mitochondrial deterioration
- nNOS inhibition improved striatal neuronal survival after 7 days recovery
- nNOS inhibition increased mature oligodendroglia in white matter tracts

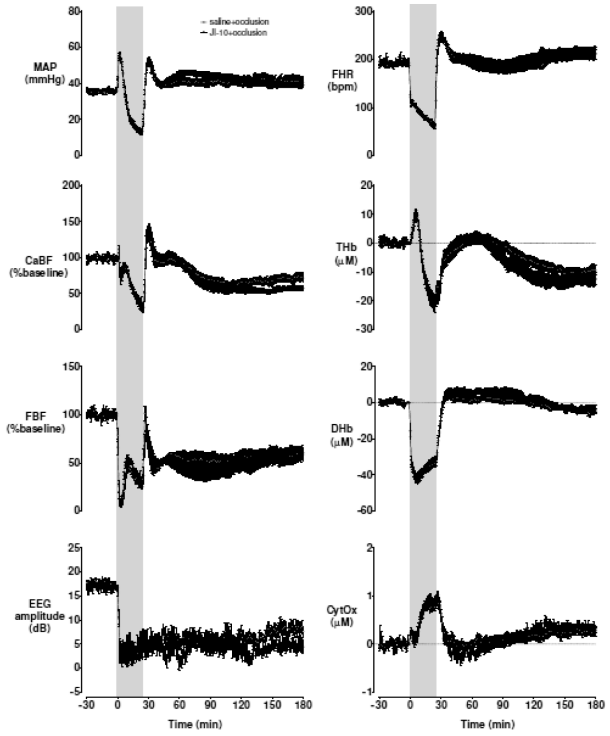

Figure 1.

Mean arterial blood pressure (MAP), fetal heart rate (FHR), carotid artery blood flow (CaBF) and conductance (CVC), femoral artery blood flow (FBF) and conductance (FVC), EEG amplitude, and NIRS derived total haemoglobin (THb), deltaHb (DHb) and cytochrome oxidase (CytOx) during baseline, 25 min complete umbilical cord occlusion (shaded) and up 155 min recovery. Time zero is the onset of occlusion. Data are minute mean±SEM.

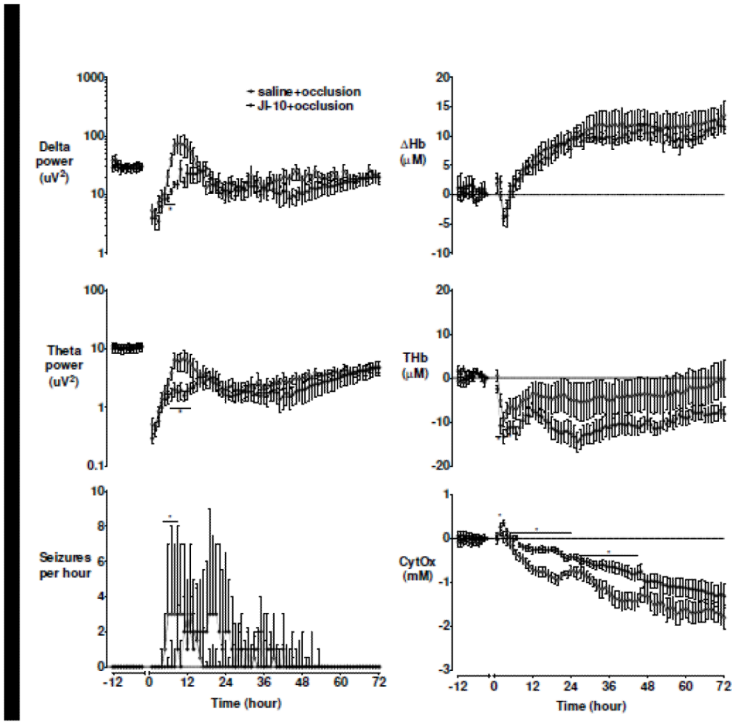

Figure 2.

Delta power, theta power, and seizures per hour on the left panel. Near-infrared spectroscopy defined deltaHb (DHb), total haemoglobin (THb) and cytochrome oxidase (CytOx) changes at baseline and during 72 h of recovery. Data are mean±SEM and compared with repeated measures ANOVA, and are median+3rd quartile for seizure data and compared with Mann-Whitney U-test. * = significant difference between groups, $p<0.05$.

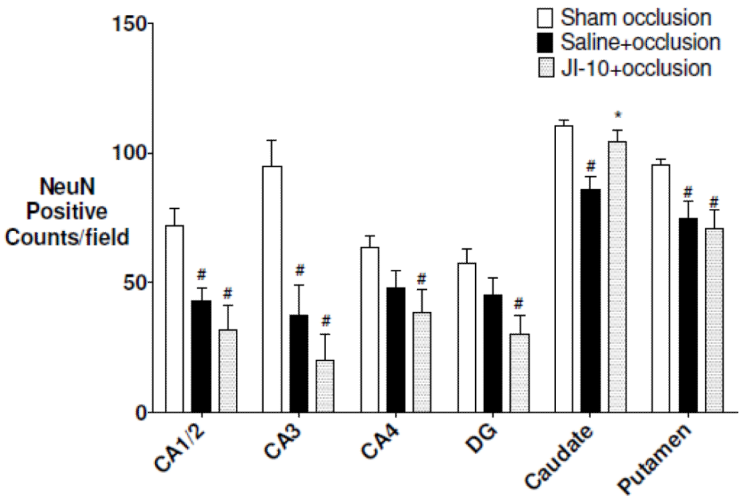

Figure 3.

NeuN cell counts after 7 d recovery. CA: cornu ammonis region; DG: dentate gyrus. Data are mean±SEM and compared with one-way ANOVA with post-hoc Tukeys pairwise comparisons. (# = significant difference from sham occlusion, $p<0.05$, * = significant difference from saline+occlusion, $p<0.05$)

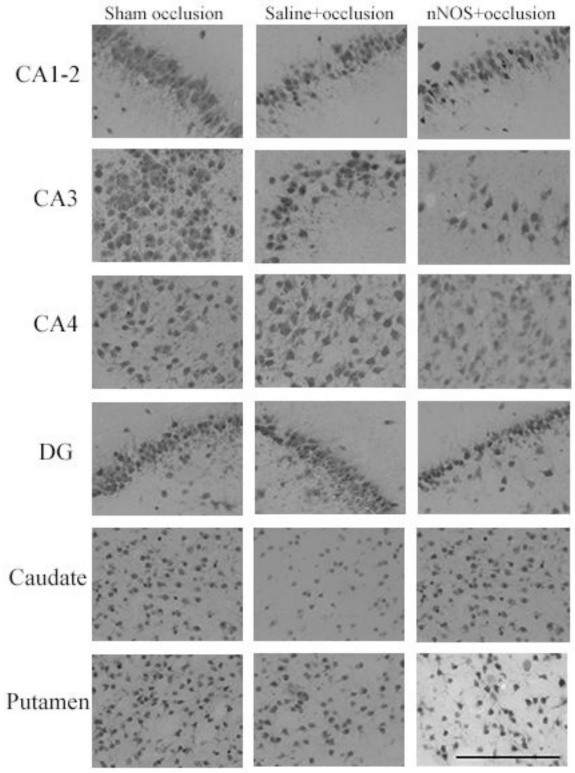

Figure 4.
Panel B: Photomicrographs showing representative NeuN immunostaining. Scale bar is 200 μm.

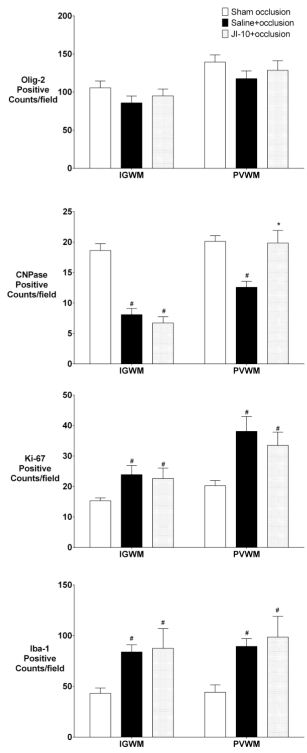

Figure 5.
Olig-2, CNPase, Ki-67 and Iba-1 cell counts after 7 d recovery. IGWM: intra-gyral white matter; PVWM: periventricular white matter. Data are mean±SEM and compared with repeated measures ANOVA with post-hoc Tukeys pairwise comparisons. comparisons (# = significant difference from sham occlusion, $p<0.05$, * = significant difference from saline +occlusion, $p<0.05$).

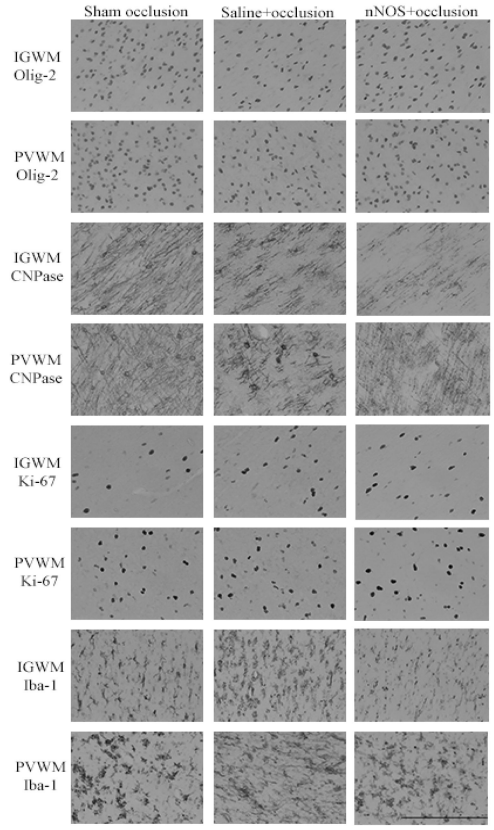

Figure 6.
Photomicrographs showing representative Olig-2, CNPase, Ki-67 and Iba-1 immunostaining. IGWM: intra-gyral white matter; PVWM: periventricular white matter. Scale bar is 200 μm.

Table 1

Arterial blood gases, glucose and lactate, and nitrite values at baseline, during 25 min umbilical cord occlusion, and for 7 days recovery.

	Group	Baseline	5min	17min	+10min	+1h	+2h	+4h	+6h	+24h	+48h	+72h	+96h	+120h	+144h	+168h
pH	Saline	7.39±0.01	7.03±0.02*	6.84±0.01*	7.16±0.01*	7.30±0.01*	7.35±0.01	7.42±0.01	7.41±0.01	7.38±0.01	7.39±0.01	7.40±0.01	7.41±0.01	7.40±0.00	7.40±0.00	7.39±0.01
	JI-10	7.38±0.01	7.04±0.01*	6.83±0.01*	7.13±0.01*#	7.28±0.02*	7.33±0.01*	7.39±0.01	7.40±0.01*	7.39±0.01	7.38±0.01	7.39±0.01	7.38±0.01#	7.38±0.00#	7.39±0.01	7.38±0.01
PCO2 (mmHg)	Saline	48.1±0.7	107.0±5.0*	142. 1±5.1*	54.6±2.1*	42.5±0.9*	43. 7±1.3*	43.0±0.5*	47.3±0.7*	46.9±0.5	47.9±1.1	47.1±0.8	46.3±1.6	47. 6±1.5	49.1±1.0	48.6±1.7
	JI-10	53.3±1.1#	107.0±3.0*	151.2±3.8*	62.7±1.7*	46.9±1.3*	45.8±0.8*	48.3±0.9*	51.1±0.9*	49.1±0.8*	50.0±1.3*	45.6±5.9	50.9±1.1	52.0±1.2	52.3±1.3	53.0±0.8
PO2 (mmHg)	Saline	24.7±1.5	6.0 ±0.9*	6.4± 0.7 *	33.3±2.0*	30.0±1.9*	25. 8±2.2	27.0±2.0	25.9±2.4	27.0±1.7	28.2±1.8*	27.3±1.7	27.8±1.6*	26. 0±1.9	26.5±2.0	26.3±2.3
	JI-10	20.7±1.3	5.0±0.7*	7.2±0.9*	29.1±1.6*	25.7±1.8*	22.2±1.8	20.9±1.7#	21.4±1.6	23.3±1.4*	24.1±1.6*	24.0±1.7*	23.3±1.8	22.5±1.5	22.7±1.5	21 1±1.4
Hb (g/dL)	Saline	10.0±0.6	11.3±0.6*	10.4 ±0. 5*	10.4±0.7	9.3±0.6	9.7 ±0.7	9.4±0.6	9.9±0.6	9.6±0. 5	9.3±0.4	9.3±0.4	9.0±0.4	9.2 ±0.3	9. 5±0.4	9.5±0.5
	JI-10	10.0±0.7	11.5±0.5*	10.9±0.7*	10.7±0.6*	10.1±0.5	9.9±0.6	10.3±0.6#	10.6±0.6#	10.3±0.5	9.9±0.4	9.8±0.5	9.8±0.6	9.7±0.6	9.7±0.7	9.8±0.8
Hct (%)	Saline	29.6±1.9	33.2±1.9*	30.5±1.5*	30.7±2.1	27.5±1.7*	28.8±2.1*	27.7±1.6	29 .2±1.6	28.2±1.4	27.3±1.1	27.3±1. 0	26 .3±1.1	27.0±0.9	27.2±1.2	28.3±1.5
	JI-10	29.4±2.0	34.0±1.6*	31.9±1.9*	31.3±1.8*	29.4±1.6	29.1±1.9	30.4±1.8	31.5±1.7*	30.5±1.6	29.3±1.3	29.0±1.5	28.9±1.8	28.8±1.8	28.4±1.9	28.7±2.4
O2ct (mmol/L)	Saline	4.0±0.4	0.5±0.0*	0. 4±0.0*	4.7±0.1	4.2±0.2	4.1±0.2	4.3±0.2	4.4±0.2	4.4±0.2	4.4±0.3	4.3±0.2	4.2±0.1	4.1±0.2	4.2±0.3	4.1±0.3
	JI-10	3.3±0.1	0.4±0.1*	0.5±0.0*	4.0±0.1*#	3.9±0.2*	3.4±0.2#	3.5±0.2#	3.9±0.2*	4.1±0.2*	3.9±0.2*	3.9±0.2*	3.8±0.2	3.7±0.2	3.7±0.2	3.5±0.2
HCO3 (mmol/L)	Saline	26.5±0.5	18.2±0.5*	13.4±0.5*	16.7±0.4*	19.6±0.5*	22.8±0.9*	26.5±0.8	28 .1±0.9	25.9±0.5	27.3±0.4	27.3±0.6	27.1±0.5	27. 1±0.5	27.7±0.5	27.0± 0.5
	JI-10	28.0±0.5	19.0±0.3*	13.9±0.5*	16.5±0.3*	20.0±0.8*	22.2±0.6*	26.6±0.5*	28.8±0.6*	27.1±0.7	26.9±0.5*	27.6±0.2	27.1±0.3	27.8±0.4	28.3±0.2	27.9±0.3
BE (mmol/L)	Saline	2.9±0.4	- 5.7±0.7*	-1 2.4 ±0.6*	-9.3±0.5*	-5.4±0.6*	- 1.5±1.0 *	2.6±0.8	4.5±0.9	2.0±0.6	3.6±0.5	3.5±0.7	3.3±0.7	3.4±0.6	4.0±0.6	3.3±0.7
	JI-10	4.7±0.5#	-4.5±0.4*	-11.7±0.5*	-9.2±0.4*	-4.8±0.9*	-1.9±0.6*	3.2±0.4*	5.6±0.6*	3.6±0.8	3.3±0.5*	4.1±0.3	3.6±0.2	4.4±0.5	4.9±0.2	4.7±0.4
Lactate (mmol/L)	Saline	1.0±0.2	4.4±0.2*	6. 8±0.4*	6.2±0.3*	4.4±0.2*	3.3±0.4*	2.3±0.4*	2.3±0.3*	1.1 ±0.1	1.0±0.1	1.0±0.1	1.0±0.1	0.9±0.1*	0.9±0.1*	0.9±0.1*
	JI-10	1.1±0.1	4.4±0.1*	7.2±0.4*	7.1±0.3*	4.8±0.2*	4.0±0.3*	2.6±0.3*	2.4±0.2*	1.9±0.4	1.2±0.1	1.3±0.2	1.3±0.3	1.2±0.1	1.1±0.1	1.1±0.1
Glucose (mmol/L)	Saline	1.0±0.1	0.4±0.1*	0. 8±0.1	1.8±0.2*	1.3±0.1*	1.4±0.2*	1.3±0.2*	1.5±0.1*	1.2±0.1	1.2±0.1*	1.1±0.1	1.1±0.1	1.1±0.0	1.1±0.1	1.1±0.1
	JI-10	1.0±0.1	0.3±0.1*	0.6±0.1*	1.6±0.1*	1.3±0.1*	1.3±0.1*	1.3±0.1*	1.5±0.1*	1.5±0.2*	1.1±0.1	1.1±0.1	1.1±0.1*	1.1±0.1	1.0±0.1	2.1 ±1.1
Nitrite (μmol/L)	Saline	0.46±0.07	0.74±0.12	0.57±0.07	0.66±0.08	0.47±0.06	0.50±0.04	0.47±0.05	0.46±0.07	0.43±0.05	0.42±0.05	0.40±0.05	0.43±0.04	0.46±0.07	0.74±0.12	0.57±0.07
	JI-10	0.43±0.04	0.81±0.10*	0.62±0.06*	0.83±0.07*	0.50±0.06	0.52±0.06	0.47±0.06	0.47±0.07	0.53±0.07	0.54±0.06	0.53±0.07	0.58±0.08	0.43±0.04	0.81±0.10	0.62±0.06

#P<0.05 compared to vehicle.

*compared to baseline. Where baseline differences exist remaining data compared with ANCOVA. Data are mean±SEM.